Wireless Pers Commun
DOI 10.1007/s11277-013-1194-9

Performance Analysis of Alamouti Space-Time Block Code Over Time-Selective Fading Channels

Van-Bien Pham · Wei-Xing Sheng

Abstract Alamouti orthogonal space-time block code (Alamouti in IEEE J Sel Areas Commun 16(8):1451–1458, 1998) has been applied widely in wireless communication, e.g., IEEE 802.16e-2005 standard. In this paper, theoretical analysis of symbol error rate performance for Alamouti orthogonal space-time block code (AOSTBC) over time-selective fading channels with a zero-forcing linear receiver is derived. Firstly, a closed-form expression (i.e., not in integral form) is derived for the average symbol pair-wise error probability (SPEP) in time-selective frequency-nonselective independent identically distributed Rayleigh fading channels. Then, the SPEP is used to derive a tight upper bound (UB) for the symbol-error rate (SER) of AOSTBC via establishing algorithmic Bonferroni-type upper bound. Extensive simulation results show that the curves for the UB coincide with the simulated SER curves for various antenna configurations even at very low signal-to-noise ratio regimes. The UB thus can be used to accurately predict the performance of AOSTBC code over time-selective fading channels when a zero-forcing receiver is used.

Keywords Space-time block code · ZF decoding · Performance analysis · Time-selective fading

1 Introduction

A simple transmit diversity scheme was proposed by Alamouti [1] for wireless communications systems. This scheme is also known as orthogonal space-time block codes for two

V.-B. Pham (✉)
Faculty of Radio-Electronics, Le Quy Don Technical University,
Hanoi, Vietnam
e-mail: bienngaxanh@gmail.com

W.-X. Sheng
Department of Communication Engineering, Nanjing University of Science and Technology, Nanjing, China
e-mail: shengwx@njust.edu.cn

Published online: 01 May 2013

transmit antennas, or AOSTBC. AOSTBC can achieve optimum decoding performance with a very simple linear maximum-likelihood (ML) decoding technique when the channel is invariant over at least two consecutive symbol durations or when the channel is quasi-static (i.e., the channel gains are invariant over the entire signaling frame but may change from frame to frame). When the channel is time-varying (i.e., the channel gains may change from symbol to symbol), the channel matrix is no longer orthogonal. This implies that the transmit antennas interfere with each other and that the linear ML decoding of AOSTBC proposed in [1] and [2] no longer offers optimum performance. On the other hand, when the channel is time-varying (i.e., the channel gains may change from symbol to symbol) then the complexity of an ML decoder of AOSTBC grows exponentially with the size of signal constellation [3]. Therefore, it is beneficial to develop low-complexity decoders for AOSTBC that can provide good performance.

The detection of AOSTBC over time-selective or fast-fading channels has been treated in [4–7]. Liu et al. [4] and Wu et al. [7] propose a simple linear near-ML decoder where the decision statistics are computed in the same way as if the channel is quasi-static by assuming that the variation between adjacent channel gains is small. Their theoretical analysis and simulation results show that the linear near-ML decoder exhibits error floors at high signal-to-noise ratio (SNR) values. To avoid exhibiting error floors, Tran et al. [5] and Vielmon et al. [6] propose a simple ZF linear decoder and decision-feedback (DF) decoder where inter-symbol interference (ISI) was completely removed. However, what this research fails to accomplish is deriving the closed-form analytical expressions for error performance. In [5], authors presented conditional error performance based on one channel realization and obtained the error performance through simulations. In [6], authors provided a closed-form analytical expression for BER. However, the result in [6] is restricted by assuming only one specific class of input signal constellation, which is binary phase-shift keying modulation, and one receiver antenna.

This paper provides theoretical analysis of symbol-error rate (SER) performance of AOSTBC over time-varying channels when a ZF decoder is used. Unlike some existing references, the error performance analysis is general and can applied for arbitrary input signal constellations and an arbitrary number of receive antennas. Firstly, the closed-form analytical expression for the symbol pair-wise error probability (SPEP) is derived. Then, the SPEP is used to derive a tight upper bound for the SER of AOSTBC via algorithmic Bonferroni-type upper bound [8]. Numerical results indicate that the SER upper bound often coincide with the true error probabilities obtained via simulations even at very low SNRs. Therefore, the SER upper bound can be used to accurately analyze the performance of AOSTBC in MIMO systems under time-varying flat fading channels (the quasi-static flat fading channel is considered as a special case).

The rest of this paper is organized as follows. The channel model and ZF decoder for AOSTBC are presented in Sect. 2. Closed-form analytical expression for the symbol pair-wise error probability (SPEP) is presented in Sect. 3. Section 4 briefly describes the algorithmic upper bound of Kuai et al. [8] and derives the exact probability expressions needed for establishing the tight upper bound. Numerical and simulation results are given in Sect. 5. Section 6 concludes the paper.

The following notations throughout are used in this paper. The superscripts $(\cdot)^{\mathrm{T}}$ denote transpose operations. $\Pr(\cdot)$ denotes probability. $E[\cdot]$ is reserved for expectation with respect to all the random variables within the braces. $x \sim \mathcal{CN}(m, \sigma^2)$ stands for circular symmetric complex Gaussian variable x with mean m and variance σ^2. $\mathrm{j} = \sqrt{-1}$.

2 Channel Model and ZF Linear Detector

2.1 Channel Model

Consider to a multiple-input multiple-output (MIMO) channel model with two transmit antennas and N receive antennas. A transmitter with two antennas employing the transmit diversity scheme of Alamouti [1] requires two signaling periods to convey a pair of finite-alphabet symbols s_1 and s_2; during the first symbol period, the symbols transmitted from antenna one and antenna two, respectively, s_1 are and s_2, and during the second symbol period they are $-s_2^*$ and s_1^*. Consider a receiver with N antennas, and assume a flat-fading channel model. Let $h_{ik}(t), i = 1, 2, k = 1, \ldots, N, t = 1, 2$ denote the equivalent complex channel coefficients between the ith transmit antenna and the kth receiver antenna during tth symbol period, so that the kth receiver observations corresponding to the two symbol periods are given by

$$\begin{cases} r_k(1) = h_{1k}(1)s_1 + h_{2k}(1)s_2 + v_k(1) \\ r_k(2) = h_{2k}(2)s_1^* - h_{1k}(2)s_2^* + v_k(2) \end{cases} \tag{1}$$

Equivalently, by conjugating the following convenient matrix representation results:

$$\underbrace{\begin{bmatrix} r_1(1) \\ r_2^*(2) \\ \vdots \\ r_N(1) \\ r_N^*(2) \end{bmatrix}}_{\boldsymbol{r}} = \underbrace{\begin{bmatrix} h_{11}(1) & h_{21}(1) \\ h_{21}^*(2) & -h_{11}^*(2) \\ \vdots & \vdots \\ h_{1N}(1) & h_{2N}(1) \\ h_{2N}^*(2) & -h_{1N}^*(2) \end{bmatrix}}_{\boldsymbol{H}} \underbrace{\begin{bmatrix} s_1 \\ s_2 \end{bmatrix}}_{\boldsymbol{s}} + \underbrace{\begin{bmatrix} v_1(1) \\ v_2^*(2) \\ \vdots \\ v_N(1) \\ v_N^*(2) \end{bmatrix}}_{\boldsymbol{v}} \tag{2}$$

or with simplified notation:

$$\boldsymbol{r} = \boldsymbol{H}\boldsymbol{s} + \boldsymbol{v} \tag{3}$$

where $\boldsymbol{v}$ represents noise. In this paper, we make the following assumptions about the channel model (3):

1. white Gaussian noise, so that $\boldsymbol{v}$ is a zero-mean circularly symmetric complex Gaussian random vector satisfying $E[\boldsymbol{v}\boldsymbol{v}^*] = N_0\boldsymbol{I}$;
2. spatially symmetric Rayleigh fading, so that, $h_{ik}(t), i = 1, 2, k = 1, \ldots, N, t = 1, 2$ is identically distributed, zero-mean unit-variance circularly symmetric complex jointly Gaussian random variables satisfying $E\left[|h_{ik}(\mathrm{t})|^2\right] = 1$;
3. sufficient antenna spacing, so that $E\left[h_{ik}(\cdot)\, h_{ml}^*(\cdot)\right] = 0$ if $i \neq m$ or $k \neq l$; relaxing this constraint would be possible, but it would complicate the analysis and it would detract from our main aim of studying the impact of time variations;
4. temporally symmetric Rayleigh fading, so that the correlation ρ between $h_{1k}(1)$ and $h_{1k}(2)$ is the same as that between $h_{2k}(1)$ and $h_{2k}(2)$, namely $E\left[h_{1k}(1)h_{1k}^*(2)\right] = E\left[h_{2k}(1)h_{2k}^*(2)\right] = \rho$;
5. perfect knowledge of $h_{ik}(t), i = 1, 2, k = 1, \ldots, N; t = 1, 2$ at the receiver

According to Jakes' model [9], we have $\rho = J_0(2\pi f_d T_s)$ where $J_0(\cdot)$ is the zeroth-order Bessel function of the first kind, f_d is the maximum Doppler shift and T_s is the period of each symbol.

2.2 Zero-Forcing (ZF) Detector

Based on the decoding method presented in [6], which is originally for the AOSTBC with one receiver antenna over time-selective fading channels, a generalized ZF decoding method for channel model (3) is introduced as follows.

Firstly, a simple matrix transformation is introduced for orthogonal combining as

$$\bar{\boldsymbol{A}} = \begin{bmatrix} -a_{22} & a_{12} \\ a_{21} & -a_{11} \end{bmatrix} \quad \text{for} \quad \boldsymbol{A} = \begin{bmatrix} a_{11} & a_{12} \\ a_{21} & a_{22} \end{bmatrix} \tag{4}$$

Then, by combining $\boldsymbol{r}$ in (3) by $\boldsymbol{\mathcal{H}} = \left[\bar{\boldsymbol{H}}_1, \bar{\boldsymbol{H}}_2, \ldots, \bar{\boldsymbol{H}}_N\right]$ with the submatrices

$$\bar{\boldsymbol{H}}_k = \begin{bmatrix} h_{2k}^*(2) & h_{2k}(1) \\ h_{1k}^*(2) & -h_{1k}(1) \end{bmatrix}; \; k = 1, 2, \ldots, N \tag{5}$$

we obtain

$$\underbrace{\boldsymbol{\mathcal{H}r}}_{\boldsymbol{y}} = \underbrace{\boldsymbol{\mathcal{H}H}}_{\boldsymbol{G}}\boldsymbol{x} + \underbrace{\boldsymbol{\mathcal{H}}v}_{\tilde{\boldsymbol{v}}} \tag{6}$$

$$\Leftrightarrow \begin{bmatrix} y_1 \\ y_2 \end{bmatrix} = \begin{bmatrix} g & 0 \\ 0 & g \end{bmatrix} \begin{bmatrix} s_1 \\ s_2 \end{bmatrix} + \begin{bmatrix} \bar{v}_1 \\ \bar{v}_2 \end{bmatrix} \tag{7}$$

with $g = \sum_{k=1}^{N} \left(h_{1k}^*(2)h_{1k}(1) + h_{2k}^*(2)h_{2k}(1)\right)$, $\bar{v}_1 \sim \mathcal{CN}(0, \alpha_1 N_0)$ and $\bar{v}_2 \sim \mathcal{CN}(0, \alpha_2 N_0)$, here $\alpha_1 = \sum_{k=1}^{N} \left(|h_{1k}(2)|^2 + |h_{2k}(1)|^2\right)$ and $\alpha_2 = \sum_{k=1}^{N} \left(|h_{2k}(2)|^2 + |h_{1k}(1)|^2\right)$, respectively. Although $\bar{v}_1$and $\bar{v}_2$ are correlated, the ZF detector ignores the correlation, and arrives at suboptimal decisions by independently quantizing y_1 and y_2.

3 Symbol Pairwise Error Probability of AOSTBC

Since the symmetry of the channel model, we only need to derive the error probability for the first symbol s_1, knowing that the second symbol will have the same error probability. From (7), the SPEP conditioned on the fading coefficients can be expressed as

$$\Pr(s \to \hat{s}|H) = \Pr\left(\left|\tilde{y} - \frac{g}{\sqrt{\alpha_1}}\hat{s}\right|^2 < \left|\tilde{y} - \frac{g}{\sqrt{\alpha_1}}s\right|^2 = |\tilde{v}|^2\right) = Q\left(\sqrt{\frac{SNR}{2}\frac{|g|^2}{\alpha_1}\Delta_s^2}\right) \tag{8}$$

where $s \to \hat{s}$ denotes a pair-wise error event, $\Delta_s^2 \triangleq \frac{|s-\hat{s}|^2}{E_s}$, $\tilde{y}$ and $\tilde{v}$ denote the normalized squared Euclidean distance, the received signal and noise signal after noise pre-whitening. Hence $\tilde{v}_1 \sim \mathcal{CN}(0, N_0)$, E_s is the total transmitted power on two transmit antennas per symbol duration and *SNR* denotes average signal-to-noise ratio at the receiver. Since the symbol pair-wise error event for each $s_i \to \hat{s}_i$ has an identical distribution, it suffices to consider the case of $s_1 \to \hat{s}_1$ for the evaluation, the subscript is dropped without loss of generality. Then, by averaging the instantaneous SPEP given in (8) over the channel realization yields the average SPEP as follows

$$\Pr(s \to \hat{s}) = \int_0^\infty Q\left(\sqrt{\omega}\right) p_W(\omega) d\omega = \int_0^\infty \frac{1}{2}\text{erfc}\left(\sqrt{\frac{\omega}{2}}\right) p_W(\omega) d\omega \tag{9}$$

where $Q(x) = \frac{1}{\sqrt{2\pi}} \int_x^\infty \exp\left(-\frac{u^2}{2}\right) du$, $\operatorname{erfc}(x) = \frac{2}{\sqrt{\pi}} \int_x^\infty \mathrm{e}^{-u^2} du$, and

$$\omega = \frac{|g|^2}{\alpha_1} \frac{SNR}{2} \Delta_s^2 \tag{10}$$

To calculate average SPEP (9), we need to derive probability density function (PDF) $p_W(\omega)$ of the random variable ω in (10).

Lemma 1 *For a channel model (3) with assumptions in Sect. 2.1, a random variable ω given in (10) has PDF*

$$p_W(\omega) = \sum_{k=0}^{2N-1} \binom{2N-1}{2N-1-k} \frac{\rho^{2k} \left(1-\rho^2\right)^{2N-1-k}}{k! c^{k+1}} \omega^k exp\left(-\frac{\omega}{c}\right) \tag{11}$$

where $\binom{n}{a} \triangleq \frac{n!}{a!(n-a)!}$ *and* $c = \frac{SNR}{2} \Delta_s^2$.

Proof The proof is given in the "Appendix".

Plugging (11) into (9) yields the average SPEP as follows

$$\begin{aligned} \Pr\left(s \to \hat{s}\right) = \frac{1}{2} \sum_{k=0}^{2N-1} \binom{2N-1}{2N-1-k} \frac{\rho^{2k} \left(1-\rho^2\right)^{2N-1-k}}{k! c^{k+1}} \\ \times \int_0^\infty \omega^k \exp\left(-\frac{\omega}{c}\right) \operatorname{erfc}\left(\sqrt{\frac{\omega}{2}}\right) p_W(\omega)\, d\omega \end{aligned} \tag{12}$$

Using equation [10, equation (6.286.1)], the average SPEP is

$$\begin{aligned} \Pr(s \to \hat{s}) = \sum_{k=0}^{2N-1} \binom{2N-1}{2N-1-k} \frac{2^k \rho^{2k} \left(1-\rho^2\right)^{2N-1-k}}{(k+1)!\, c^{k+1}} \frac{\Gamma\left(\frac{2k+3}{2}\right)}{\sqrt{\pi}} {}_2F_1 \\ \times \left(k+1, k+\frac{3}{2}; k+2; -\frac{2}{c}\right) \end{aligned} \tag{13}$$

$$\begin{aligned} \Pr(s \to \hat{s}) = \frac{\left(1-\rho^2\right)^{2N-1}}{2c} {}_2F_1\left(1, \frac{3}{2}; 2; -\frac{2}{c}\right) + \frac{2^{2N-1} \rho^{4N-2}}{(2N)!\, c^{2N}} \frac{\Gamma\left(\frac{4N+1}{2}\right)}{\sqrt{\pi}} {}_2F_1 \\ \times \left(2N, 2N+\frac{1}{2}; 2N+1; -\frac{2}{c}\right) + \sum_{k=1}^{2N-2} \binom{2N-1}{2N-1-k} \\ \times \frac{2^k \rho^{2k} \left(1-\rho^2\right)^{2N-1-k}}{(k+1)!\, c^{k+1}} \frac{\Gamma\left(\frac{2k+3}{2}\right)}{\sqrt{\pi}} {}_2F_1\left(k+1, k+\frac{3}{2}; k+2; -\frac{2}{c}\right) \end{aligned} \tag{14}$$

where and $\Gamma(\cdot)$ is a Gamma function ${}_2F_1(a, b; c; z)$ is a Hypergeometric function which provided in common mathematical software, such as MATHEMATICAL, MAPLE, etc.

We also emphasize that the derivation given in (14) is closed-form for arbitrary constellation $\mathcal{A}$ and arbitrary number of receiver antenna N. From generalized Eq. (14), it is easy

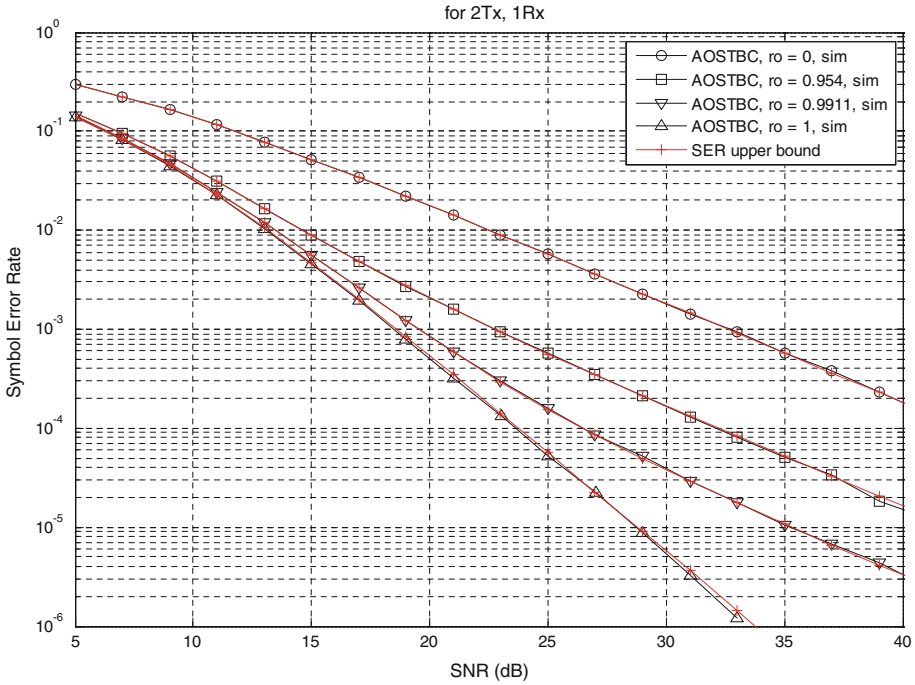

Fig. 1 Comparison of the upper bound and simulated SER of AOSTBC with different correlated factors for one receive antenna ($N = 1$). In this figure, the correlation factor ρ is denoted as ro

to obtain average SPEP on two extreme cases: the quasi-static fading channel ($\rho = 1$) and the fast fading channel ($\rho = 0$).

Special case 1: For quasi-static fading channel ($\rho = 1$)

$$\Pr\left(s \to \hat{s}\right) = \frac{2^{2N-1}}{(2N)\,!c^{2N}} \frac{\Gamma\left(\frac{4N+1}{2}\right)}{\sqrt{\pi}} {}_2F_1\left(2N, 2N + \frac{1}{2}; 2N + 1; -\frac{2}{c}\right) \tag{15}$$

Special case 2: For fast fading channel ($\rho = 0$)

$$\Pr\left(s \to \hat{s}\right) = \frac{1}{2c}\, {}_2F_1\left(1, \frac{3}{2}; 2; -\frac{2}{c}\right) \tag{16}$$

From (16) we conclude that when the channel is fast fading (channel gains change independently from symbol to symbol), then increasing number of receiver antenna also does not come with any performance improvement for ZF detectors. This conclusion is confirmed by simulation results in Figs. 1 and 2.

4 Tight Upper Bound on the SER

In this section we apply the greedy algorithm in [8] for a tight Bonferroni-type upper bound to achieve a tight error bound for AOSTBC over time-selective frequence-nonselective Rayleigh fading channels.

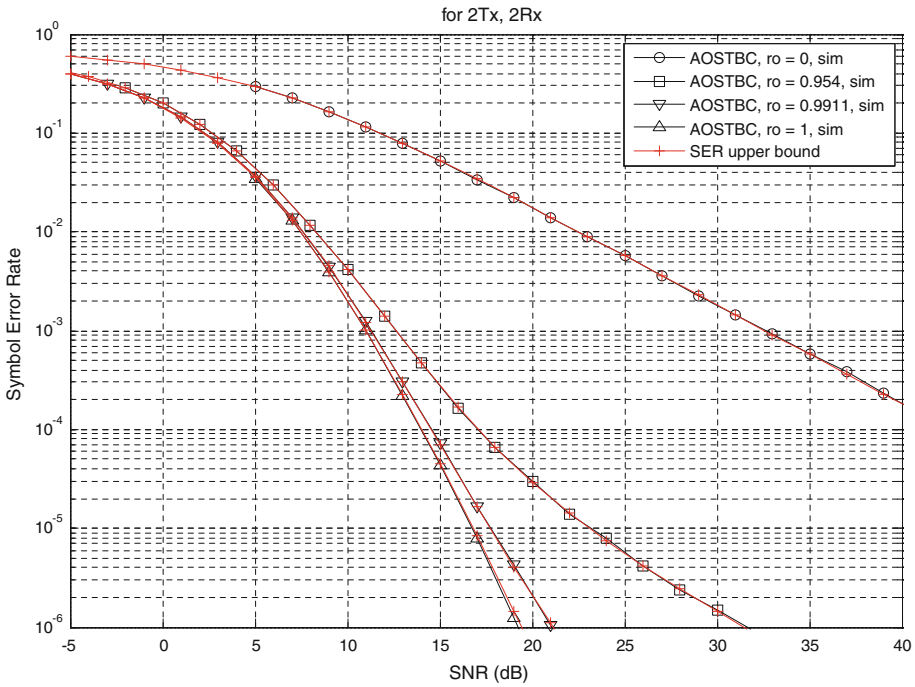

Fig. 2 Comparison of the upper bound and simulated SER of AOSTBC with different correlated factors for two receive antennas ($N = 2$). In this figure, the correlation factor ρ is denoted as ro

4.1 The Bonferroni-Type Upper Bound

For a positive integer M, let $A_1, A_2, \ldots, A_M$ be events in an arbitrary probability space. A greedy algorithm is given in [8] to find a upper bound for the probability of the union of the A_i. The bound is given by

$$P\left(\bigcup_{i=1}^{M} A_i\right) \leq \sum_{i=1}^{M} P\left(A_i\right) - \max_{T_0 \in T} \sum_{(i,j)\in T_0} P\left(A_i \bigcap A_j\right) \tag{17}$$

where T is the set of all spanning trees of the M indices, i.e., the trees whose set of nodes is the set of indexes $\{1, 2, \ldots, M\}$. The greedy algorithm in [8] is as follows. First, each pair of nodes (i, j) is connected via edges of weight $P\left(A_i \bigcap A_j\right)$ to form a fully connected graph. To form the tree T_0, the algorithm starts from the edge with the largest weight (the (i, j) with the largest $P\left(A_i \bigcap A_j\right)$. Then, at each step, the edge with the largest weight is added to T_0, subject to the constraint that there is no cycle in T_0. This step is executed until all of the nodes are in T_0.

4.2 Tight Upper Bound of Symbol Error Rate

For a constellation $\mathcal{A}$ of size M, the SER is given by [11]

$$\text{SER} = \sum_{u=1}^{M} P\left(\varepsilon \,|s_u\right) P\left(s_u\right) = \frac{1}{M} \sum_{u=1}^{M} P\left(\bigcup_{i\neq u} \varepsilon_{iu}\right) \tag{18}$$

where $P(\cdot|s_u) \triangleq P_u(\cdot)$ is the conditional probability of error given that s_u was sent, and ε_{iu} indicates the error event $s_u \to s_i$. Note that $P_u(\varepsilon_{iu})$ is the average SPEP and is given in (14). In order to find upper bound on the probability of each union in (18) via (17), we need to find the probability of the intersection of ε_{iu} and ε_{ju}, the two-dimension (2-D) SPEP of symbols s_i and s_j with s_u. From (8), the SPEP conditioned on the fading coefficients can be rewritten as

$$P(s_i \to s_j|\boldsymbol{H}) = Q\left(\delta_{ij}\sqrt{Z}\right) \tag{19}$$

where $\delta_{ij} = \sqrt{\frac{SNR}{2}\Delta_{ij}^2}$, $\Delta_{ij}^2 = \frac{|s_i - s_j|^2}{E_s}$ and

$$Z = \frac{|g|}{\sqrt{\alpha_1}} \tag{20}$$

From Lemma 1, letting $c = 1$ we easily have PDF of random variable Z as

$$p_Z(z) = \sum_{k=0}^{2N-1} \binom{2N-1}{2N-1-k} \frac{\rho^{2k}\left(1-\rho^2\right)^{2N-1-k}}{k!} z^k \mathrm{e}^{-z} \tag{21}$$

Thus, the 2-D SPEP of symbols s_i and s_j with s_u can be done by averaging [8, equation (7)], i.e.,

$$P_u\left(\varepsilon_{iu} \bigcap \varepsilon_{ju}\right) = E_Z\left[\psi\left(\mu_{iju}, \delta_{iu}\sqrt{Z}, \delta_{ju}\sqrt{Z}\right)\right] \tag{22}$$

where $\mu_{iju} = \frac{\langle s_i - s_u, s_j - s_u\rangle}{d_{iu}d_{ju}}$, $\langle x, y\rangle = \Re(x)\Re(y) + \Im(x)\Im(y)$ ($\Re(\cdot)$ and $\Im(\cdot)$ are the real and imaginary parts, respectively), $d_{iu} = |s_i - s_u|$, Z is defined in (20) and $\psi\left(\rho, \delta_{iu}\sqrt{Z}, \delta_{ju}\sqrt{Z}\right)$ given by [11, equation (11)] as

$$\begin{aligned}\psi\left(\mu, \delta_{iu}\sqrt{Z}, \delta_{ju}\sqrt{Z}\right) = \frac{1}{2\pi}\int_0^{\varphi(d_{iu}/d_{ju},\mu)} \exp\left(-\frac{\delta_{iu}^2}{2\sin\theta}z\right)d\theta \\ + \frac{1}{2\pi}\int_0^{\varphi(d_{ju}/d_{iu},\mu)} \exp\left(-\frac{\delta_{ju}^2}{2\sin\theta}z\right)d\theta\end{aligned} \tag{23}$$

where $\varphi(x,\mu) = \tan^{-1}\left(x\sqrt{1-\mu^2}/(1-\mu x)\right)$, and $\tan^{-1}(x)$ is defined here as $\pi - \tan^{-1}(-x)$ for negative x. By using the PDF of Z in (21), we find the expected value of each of the integrals in (23) as follows:

$$E_Z\left[\int_0^{\varphi} \mathrm{e}^{-a(\theta)Z}d\theta\right] = \int_0^{\varphi}\int_0^{\infty} \mathrm{e}^{-a(\theta)z}p_Z(z)dzd\theta \tag{24}$$

$$E_Z\left[\int_0^{\varphi} \mathrm{e}^{-a(\theta)Z}d\theta\right] = \int_0^{\varphi}\sum_{k=0}^{2N-1}\binom{2N-1}{2N-1-k}\frac{\rho^{2k}\left(1-\rho^2\right)^{2N-1-k}}{k!}\int_0^{\infty} z^k\mathrm{e}^{-(1+a(\theta))z}dzd\theta \tag{25}$$

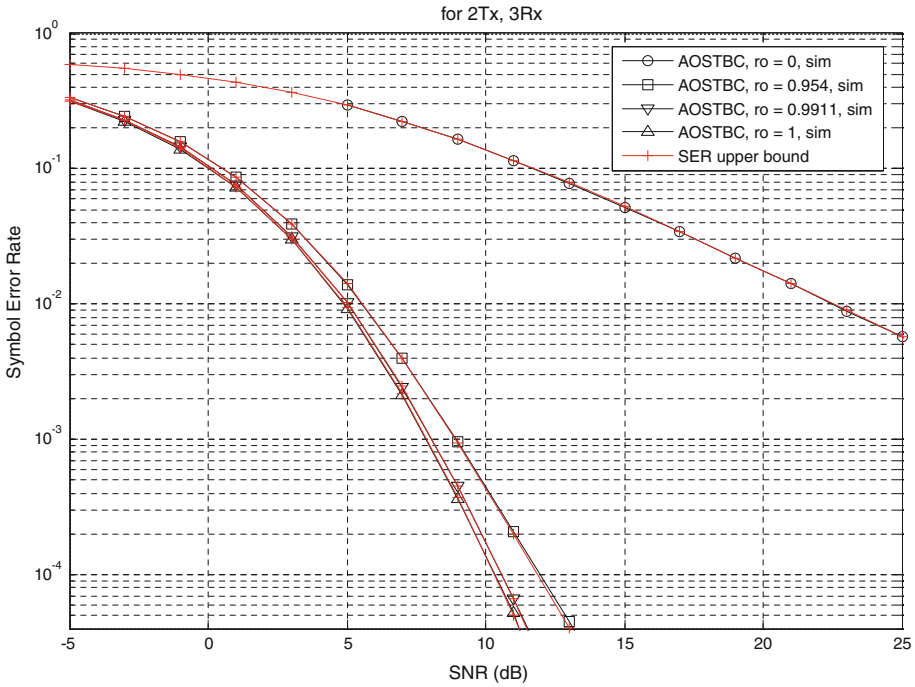

Fig. 3 Comparison of the upper bound and simulated SER of AOSTBC with different correlated factors for three receive antennas ($N = 3$). In this figure, the correlation factor ρ is denoted as ro

By noticing in [10, equation (3.351.1)] that $\int_0^\infty x^n \mathrm{e}^{-\alpha x} dx = n!\alpha^{-n-1}$, the Eq. (25) can be written as

$$E_Z\left[\int_0^{\varphi} \mathrm{e}^{-a(\theta)Z} d\theta\right] = \sum_{k=0}^{2N-1} \binom{2N-1}{2N-1-k} \rho^{2k} \left(1-\rho^2\right)^{2N-1-k} \int_0^{\varphi} \left(\frac{1}{1+a(\theta)}\right)^{k+1} d\theta \tag{26}$$

By using Eq. (26) with $a(\theta) = \frac{\delta^2}{2\sin\theta}$ and [11, equation (14)], we have

$$I(\varphi,\delta) = \sum_{k=0}^{2N-1} \binom{2N-1}{2N-1-k} \frac{\rho^{2k}\left(1-\rho^2\right)^{2N-1-k}}{2\pi} \left[\varphi - \frac{\beta\delta}{\sqrt{2+\delta^2}} \sum_{n=0}^{k} \binom{2n}{n} \frac{1}{2^n\left(2+\delta^2\right)^n} - \frac{\delta}{\sqrt{2+\delta^2}} \sum_{n=0}^{k} \sum_{m=0}^{n-1} \binom{2n}{m} \frac{(-1)^{n+m}}{2^n\left(2+\delta^2\right)^n} \frac{\sin(2\beta(n-m))}{n-m}\right] \tag{27}$$

where $\beta = \frac{1}{2}\tan^{-1}\frac{A}{B} + \frac{\pi}{2}\left[1 - \frac{1+\mathrm{sign}B}{2}\mathrm{sign}A\right]$, $A = \delta\sqrt{2+\delta^2}\sin 2\varphi$, $B = \left(1+\delta^2\right)\cos 2\varphi - 1$ and $\mathrm{sign}A \triangleq |A|/A$ if $A \neq 0$ and 0 otherwise. Therefore, from Eqs. (22), (23), and (27), we obtain the following expression for the 2-D SPEP

$$P_u\left(\varepsilon_{iu} \bigcap \varepsilon_{ju}\right) = I\left(\varphi\left(\frac{\delta_{iu}}{\delta_{ju}}, \mu_{iju}\right), \delta_{iu}\right) + I\left(\varphi\left(\frac{\delta_{ju}}{\delta_{iu}}, \mu_{iju}\right), \delta_{ju}\right) \tag{28}$$

Finally, plugging Eqs. (17), (14) and (28) into Eq. (18) we obtain a tight upper bound for SER.

5 Simulation Results

In order to check the accuracy of the theoretical error analysis, we have carried out Monte-Carlo simulations for ZF detector (7) with channel model (3) and then compared them with the theoretical analysis. Two typical Doppler spreads in this section are $f_d T_s = 0.03$ ($\rho = 0.9911$) and $f_d T_s = 0.0687 (\rho = 0.954)$. Two typical Doppler spreads correspond to a 1.9 GHz personal communications services (PCS) system, in which the symbol rate is 6.4 kBd and the speed of the mobile is 112 and 250 km/h. Two extreme cases: the quasi-static channel ($\rho = 1$) and the fast fading channel ($\rho = 0$) are also considered. The SER versus SNR curves are presented in Figs. 1 and 2 for various N and 4-QAM constellations.

Figures 1, 2 and 3 present comparisons between simulation results and theoretical analysis for $N = 1$, 2 and 3 receive antennas. The exact SER curves are obtained by Monte-Carlo simulations over 10^8 independent channel realizations and the curves for the union bound on the SER are performed by Eq. (18). These figures show our upper bound is very tight for any value of ρ and arbitrary number of receiver antenna at all SNR values. This demonstrates that theoretical UB on the SER is exact and coincides (within 0.01 dB) with the simulated SER for various fading parameters and different antenna configurations. Similar results can be found for different constellations; details are omitted for brevity.

6 Conclusions

This paper investigated the SER of AOSTBC code over time-selective fading with a zero-forcing linear receiver. A very tight upper bound on the SER was developed. This bound is applicable for arbitrary constellations and mappings for arbitrary number of receive antennas. This bound also can provide practically the exact SER over a wide range of the SNR. The studies in this paper therefore provide a very effective tool to predict the SER performances of AOSTBC code over time-selective fading channels with a zero-forcing linear receiver without the need of time-consuming simulations.

Acknowledgments This work was partially supported under Project 39/2012/HĐ/NĐT granted by the Ministry of Science and Technology of Vietnam.

Appendix

Assume that $\rho^2 < 1$, let us introduce the random variables ε_{1k} and ε_{2k}, $k = 1, \ldots, N$

$$\xi_{1k} = \frac{h_{1k}(1) - \rho h_{1k}(2)}{\sqrt{1-\rho^2}}; \xi_{2k} = \frac{h_{2k}(2) - \rho h_{2k}(1)}{\sqrt{1-\rho^2}} \tag{29}$$

By construction, ε_{1k} and ε_{2k} are independent and identically distributed with the same PDF as $h_{1k}(2)$ and $h_{2k}(1)$, and furthermore, ε_{1k} is independent of $h_{1k}(2)$, ε_{2k} and is independent of $h_{2k}(1)$. Plugging (29) into (10) leads to

$$\omega = \left| \rho\sqrt{\alpha_1} + \sqrt{1-\rho^2} \frac{\sum_{k=1}^{N} \left(h_{1k}^*(2)\, \xi_{1k} + h_{2k}(1)\, \xi_{2k}^* \right)}{\sqrt{\alpha_1}} \right|^2 \frac{SNR}{2} \Delta_s^2 \tag{30}$$

To simplify this expression further, observe that the fraction in (30) can be expressed as an inner product

$$z_1 + \mathrm{j}z_2 = \frac{\sum_{k=1}^{N} \left(h_{1k}^* (2)\, \xi_{1k} + h_{2k} (1)\, \xi_{2k}^* \right)}{\sqrt{\alpha_1}} = \left\langle \frac{\boldsymbol{h}}{\|\boldsymbol{h}\|}, \boldsymbol{e} \right\rangle \tag{31}$$

where z_1, z_2 are real variables, $\boldsymbol{h} = \left[h_{11} (2), h_{21}^* (1), \ldots, h_{1N} (2), h_{2N}^* (1) \right]^{\mathrm{T}}$ and $\boldsymbol{e} = \left[\xi_{11}^*, \xi_{21}, \ldots, \xi_{1N}^*, \xi_{2N} \right]^{\mathrm{T}}$. Since $\boldsymbol{e}$ is symmetric, the distribution of $z_1 + \mathrm{j}z_2$ reduces to the distribution of $h_{1k}(1)$, independent of $\boldsymbol{h}$ (and, thus, also independent of $\|\boldsymbol{h}\|$). Thus, (30) simplifies to

$$\omega = \left| \rho \sqrt{\alpha_1} + \sqrt{1 - \rho^2}\, (z_1 + \mathrm{j}z_2) \right|^2 \frac{SNR}{2} \Delta_s^2 \tag{32}$$

$$\omega = (A + X_1)^2 + X_2^2 \tag{33}$$

where $A = \sqrt{\alpha_1 \frac{\rho^2 SNR}{2} \Delta_s^2}$ and $X_i = \sqrt{\left(1 - \rho^2\right) \frac{SNR}{2} \Delta_s^2} z_i$. Therefore, given A, ω has a noncentral chi-square distribution with two degrees of freedom, and PDF

$$p_{W|A}\, (\omega \,|a\,) = \frac{1}{\left(1 - \rho^2\right) c} \exp\left(-\frac{\omega + a^2}{\left(1 - \rho^2\right) c} \right) J_0 \left(\frac{2\mathrm{j}a}{\left(1 - \rho^2\right) c} \sqrt{\omega} \right) \tag{34}$$

where $J_0(\cdot)$ is the zeroth-order Bessel function of the first kind, $c = \frac{SNR}{2} \Delta_s^2$ and $\mathrm{j} = \sqrt{-1}$.

However, $A = \sqrt{\alpha_1 \frac{\rho^2 SNR}{2} \Delta_s^2} = \sqrt{\alpha_1 \rho^2 c}$ is Rayleigh distributed with $2N$ degrees of freedom, and PDF

$$p_A\, (a) = \frac{2}{\rho^{4N} c^{2N} \Gamma\, (2N)} a^{4N-1} \exp\left(-\frac{a^2}{\rho^2 c} \right) \tag{35}$$

Integrating the product of (34) and (35) over the variable from 0 to ∞ leads to the following density probability for ω as

$$p_W\, (\omega) = \int_0^\infty p_{W|A}\, (\omega \,|a\,) p_A\, (a)\, da \tag{36}$$

$$\begin{aligned} p_W\, (\omega) = {} & \frac{2}{\left(1 - \rho^2\right) \rho^{4N} c^{2N+1} \Gamma\, (2N)} \exp\left(-\frac{\omega}{\left(1 - \rho^2\right) c} \right) \\ & \times \int_0^\infty a^{4N-1} \exp\left(-\frac{a^2}{\left(1 - \rho^2\right) \rho^2 c} \right) J_0 \left(\frac{2\mathrm{j}\sqrt{\omega}}{\left(1 - \rho^2\right) c} a \right) da \end{aligned} \tag{37}$$

From (37), by using [10, Eq. (6.631.1)] we obtain

$$p_W\, (\omega) = \frac{\left(1 - \rho^2\right)^{2N-1}}{c} \exp\left(-\frac{\omega}{\left(1 - \rho^2\right) c} \right) {}_1F_1 \left(2N, 1; \frac{\rho^2}{\left(1 - \rho^2\right) c} \omega \right) \tag{38}$$

where ${}_1F_1(\alpha, \beta; z)$ is Kummer confluent hypergeometric function [10]. By applying the transform equations given in [12,13] we have

$$ {}_1F_1\left(2N, 1; \frac{\rho^2}{(1-\rho^2)c}\omega\right) = \exp\left(\frac{\rho^2\omega}{(1-\rho^2)c}\right)\sum_{k=0}^{2N-1}\binom{2N-1}{2N-1-k}\frac{\rho^{2k}}{k!\,(1-\rho^2)^k\,c^k}\omega^k \tag{39} $$

Plugging (39) into (38) leads to

$$ p_W(\omega) = \sum_{k=0}^{2N-1}\binom{2N-1}{2N-1-k}\frac{\rho^{2k}\left(1-\rho^2\right)^{2N-1-k}}{k!c^{k+1}}\omega^k\exp\left(-\frac{\omega}{c}\right) \tag{40} $$

It is very interesting that the calculation process from (29) to (40) is performed under assumption $\rho^2 < 1$. However, the final result (40) is general and can apply any value of ρ (which includes $\rho^2 = 1$). The proof is not difficult, so it is omitted here for brevity.

References

1. Alamouti, S. M. (1998). A simple transmitter diversity scheme for wireless communications. *IEEE Journal on Selected Areas in Communication*, *16*(8), 1451–1458.
2. Tarokh, V., Seshadri, N., & Calderbank, A. R. (1998). Space-time block coding for wireless communications: Performance results. *IEEE Journal on Selected Areas in Communication*, *17*(3), 451–460.
3. Naguib, A. F., Seshadri, N., & Calderbank, A. R. (1998). Applications of space-time block codes and interference suppression for high capacity and high data rate wireless systems. In *Systems and computers: Conference record of thirty-second asilomar conference on signals*, pp. 1803–1810.
4. Liu, Z., Ma, X., & Giannakis, G. B. (2002). Space-time coding and Kalman filtering for time-selective fading channels. *IEEE Transactions on Communications*, *50*(2), 183–186.
5. Tran, T. A., & Sesay, A. B. (2004). A generalised simplified ML decoder of orthogonal space-time block code for wireless communications over time-selective fading channels. *IEEE Transactions on Wireless Communications*, *3*(3), 855–964.
6. Vielmon, A., Li, Y. (G.), & Barry J. R. (2004). Performance of Alamouti transmit diversity over time-varying Rayleigh-fading channels. *IEEE Transactions on Wireless Communications, 3*(5), 1369–1373.
7. Wu, J., & Saulnier, G. J. (2007). Orthogonal space-time block code over time-varying flat-fading channels: Channel estimation, detection, and performance analysis. *IEEE Transactions on Wireless Communications*, *55*(5), 1077–1087.
8. Kuai, H., Alajaji, F., & Takahara, G. (2000). Tight error bounds for non-uniform signaling over AWGN channels. *IEEE Transactions on Information Theory*, *46*(11), 2712–2718.
9. Jakes, W. C. (1974). *Microwave mobile communication*. New York: Wiley.
10. Gradshteyn, I. S., & Ryzhik, I. M. (2007). *Table of integrals, series, and products* (7th ed.). San Diego, CA: Academic.
11. Behnamfar, F., Alajaji, F., & Linder, T. (2005). Tight error bounds for space-time orthogonal block codes under slow Rayleigh flat fading. *IEEE Transactions on Wireless Communications*, *53*(6), 952–956.
12. http://functions.wolfram.com/HypergeometricFunctions/Hypergeometric1F1/03/01/02/0011/. Accessed 28 March 2013.
13. http://functions.wolfram.com/HypergeometricFunctions/LaguerreL3General/06/01/03/01/02/0001/. Accessed 28 March 2013.

Author Biographies

Van-Bien Pham was born in Hanoi, Vietnam in November 1978. He received his B.S. and M.S. degrees in electronic engineering from Le Quy Don Technical University, Hanoi, Vietnam in 2002 and 2005, and his Ph.D. degree in information and communication engineering from Nanjing University of Science and Technology, Nanjing, China in 2012. Now, he is a lecturer at Faculty of Radio-Electronics, Le Quy Don Technical University, Hanoi, Vietnam. His research interests include MIMO wireless communication, cognitive radio, network coding, cooperative communication and space-time coding.

Wei-Xing Sheng was born in Jiangsu, China in November 1966. He received the B.Sc. M.S. and Ph.D. degrees in electronic engineering from Shanghai Jiaotong University, Nanjing University of Science and Technology in 1988, 1991 and 2002 respectively. Since 1991, he has been with Nanjing University of Science and Technology where he is currently a professor in department of communication engineering. His research interests include array antenna, array signal processing and signal processing in radar or communication systems.